New ^{237}Np Burning Strategy in a Supercritical CO_2 Cooled Fast Reactor Core Attaining Zero Burnup Reactivity Loss

Hoai Nam Tran and Yasuyoshi Kato
Research Laboratory for Nuclear Reactors, N1-2, Tokyo Institute of Technology
O-okayama, Meguro-ku, Tokyo 152-8550, JAPAN
Email: 05d51395@nr.titech.ac.jp

Abstract

A new ^{237}Np burning strategy in a supercritical CO_2 cooled fast reactor core is proposed, which consumes ^{237}Np as fuel and utilizes it as a burnable poison to attain zero burnup reactivity loss. Addition of ^{237}Np at content of 6.5 weight percent in fuel engenders essentially zero burnup reactivity loss of the rate of 0.02% $\Delta k/k$ over ten years and consumption of the equivalent quantity produced from about 14 light-water reactors of equivalent electrical output. The zero burnup reactivity loss results in reduction of the control rod number to half that of a usual sodium-cooled mixed oxide fuel core with no added ^{237}Np and no need for rod operation with fuel burning. Void reactivity is smaller by 25% than that of the usual core, although ^{237}Np is added and the active core length is elongated to 1.2 m. The power density is reduced to about 1/5 of that of a usual core and the hot spot temperature of cladding is below its maximum permissible temperature of 700°C.

KEYWORDS: fast reactor, reactivity loss, core design, minor actinide, neptunium, CO_2

1. Introduction

Sodium is currently used as coolant in fast reactors (FRs) to provide efficient heat removal of the tight fuel pin lattice aimed at attaining a harder neutron spectrum and higher breeding gain. However, some undesirable features of sodium use include:

1) Positive sodium void reactivity
2) Hazardous (chemical) reaction with water or air in the event of sodium leakage
3) Higher capital cost mainly caused by the need for more intermediate cooling loops than light-water reactors (LWRs)

Use of gas as a coolant can eliminate problems 1) and 2) above. Nevertheless, generally, gas has poor heat transport properties relative to sodium. To provide sufficient core cooling, gas must be pressurized to 10–20 MPa, whereas sodium systems operate at atmospheric pressure. One direct consequence of this requirement of high pressure is the necessary assurance that the core can be cooled safely at reduced pressures that might result from accidental depressurization.

Use of several gas coolants, including steam, carbon dioxide, and helium, have been examined in past studies [1]. Steam has been rejected because of its low breeding ratio and excessive cladding corrosion. Carbon-dioxide-cooled and helium-cooled fast reactors have been studied primarily in the UK, US, and Germany.

Salient advantages of using carbon dioxide and helium as coolants of fast reactors instead of sodium are [1], [2]:

1) A harder neutron spectrum giving a small burn-up reactivity swing, low core-excess

reactivity control requirements, and more efficient burning of minor actinides (MAs).

2) Considerably low coolant void reactivity improvement beyond design-base accident event consequences, especially for minor actinide burning cores, giving more flexibility on core geometrical design, especially core height.
3) Inertness to water or air, thereby eliminating dedicated systems that ensure safety in sodium-cooled fast reactors.
4) Transparency of coolant, allowing ease of inspection and maintenance.
5) Non-activating coolant, eliminating intermediate loops and leading to lower capital costs.
6) Gas phase coolant in the core, causing no mechanical damage from molten fuel and + coolant interaction during unprotected accident conditions.

Cycle efficiency decreases with lowered turbine inlet temperature more slowly in carbon dioxide (CO_2) gas turbine cycles than in helium (He) gas turbine cycles. The efficiency of the CO_2 cycle is greater than 40% at a representative core outlet temperature of fast reactors (530°C), whereas the efficiency is around 30% in He cycles [3]–[5]. The turbine size of the CO_2 cycles is about five times smaller than that of the He cycles [6], [7].

As a cooling medium, CO_2 has preferable properties to those of He [4]. The heat transfer coefficient h between the coolant and fuel cladding surface is calculated as

$$h = Nu\ (\lambda/d)$$
$$\propto (Re^{0.8}\ Pr^{0.4})\ (\lambda/d),$$

where Nu = Nusselt number, λ = heat conductivity, d = hydraulic equivalent diameter, Re = Reynolds number and Pr = Prandtl number. The above equation provides a 1.5 times higher heat transfer coefficient h in CO_2 at the same gas velocity, leading to a smaller temperature difference between the coolant and fuel rod cladding surface by a factor of about 1.5 in CO_2 relative to that in He. The higher heat transport capacity, measured as a product of specific heat at constant pressure Cp and molecular weight M, gives about 2.5 times more effective core decay heat removal under natural circulation conditions than He. The 3.6-times longer depressurization time of CO_2 and higher heat transport capacity (mentioned above) over that of He mitigates the depressurization transient and simplifies design of the passive decay heat removal system described later. Carbon dioxide is about 250 times less expensive than He per unit weight and 24 times less expensive per unit volume. In addition, considering lower leakage rate characteristics of CO_2 than He, coolant leakage problems of gas cooled reactors in operation are orders of magnitude less severe than with He.

In short, the CO_2 gas turbine FR offers an alternative to sodium-cooled FRs, eliminating problems related to safety, plant maintenance and construction cost.

Main nuclides associated with geological disposal of long-lived radioactive wastes in nuclear power generation consist of a small number of long-lived MAs (mostly ^{237}Np, ^{241}Am, and ^{243}Am) and fission products (^{99}Tc and ^{129}I). The MAs can be transmuted to stable or shorter half-life isotopes through nuclear fission. This process is most efficient in a hard neutron spectrum that minimizes production of other higher minor actinides through neutron capture reactions. The CO_2 direct cycle provides a harder neutron spectrum in the core than a usual sodium-cooled FR because of weaker moderating properties of the CO_2 coolant, transmuting the minor actinides more efficiently. It not only reduces repository risks of the minor actinides with high radiological toxicity; it also

conserves uranium resources through use of the minor actinides as fuel. Long lived fission products (^{99}Tc and ^{129}I) are transmuted efficiently to stable isotopes (^{100}Ru and ^{130}Xe) in a moderated neutron spectrum to take advantage of resonance and thermal absorptions in these isotopes.

A PWR with an electrical output of 1000 MWe and average discharge burnup of 33 GWd/MT produces about 24 kg of MAs at three years after fuel discharge. Neptunium-237 comprises about 40–60% of the total MAs discharged from PWRs and BWRs. It is also a main nuclide of geological disposal of long-lived radioactive wastes. In FRs, especially in gas-cooled FRs, MAs are useful as burnable poison by taking advantage of their hard neutron spectrum to minimize burnup reactivity loss and extend the core lifetime while reducing long-lived wastes [8], [9]. A major difficulty in using substantial quantities of MAs is the considerable increase in void reactivity because ^{237}Np and ^{241}Am have threshold fission cross-sections that engender a significant response to neutron spectral hardening associated with coolant-voiding. However, void reactivity of a CO_2 cooled core with 1.2 m core height is about 25% less than that of a usual sodium-cooled core such as of MONJU with 0.93 m core height as described later. Therefore, void reactivity would be less restrictive in a GCFR core than in sodium-cooled core.

Extensive studies have been undertaken of the transmutation rate of the long-lived MAs and fission products [10]–[11]. Most studies have specifically addressed the transmutation rate and the effect on safety parameters such as increase of void reactivity and decrease of the Doppler coefficient. In this study, an effort was made to pursue simultaneous burning of ^{237}Np as fuel and improvement of the core neutronics performance to attain zero burnup reactivity loss through use as a burnable poison.

2. Calculations and results

A supercritical CO_2 gas turbine FR core with an electricity output of 244 MWe, which has two regions of plutonium enrichment, has been designed. Respective levels of plutonium enrichment of the inner and outer part of the core are 14.7 and 20.0 atom%. The inner and outer parts of the core respectively contain 159 subassemblies and 102 subassemblies. The core height and equivalent diameter are, respectively, about 1.2 m and about 3.146 m. Details of core parameters and configurations are shown in Table 1 and Fig. 1.

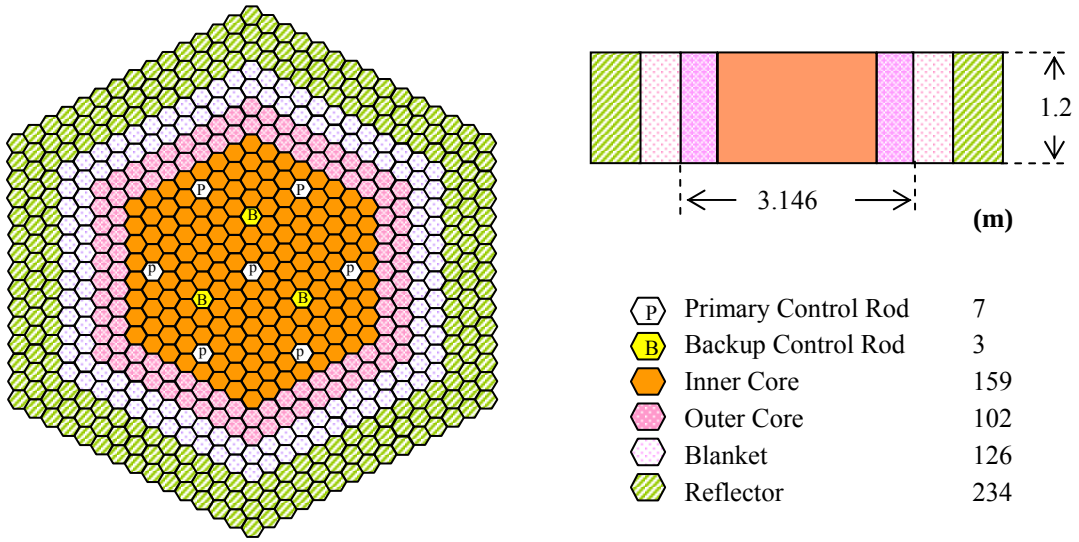

Figure 1: Configuration of a supercritical CO_2-cooled fast reactor core

Neutronic calculations were done in a three-dimensional triangular-z geometry using a seven-group cross section set prepared from JENDLE-3.2 and CITATION neutron diffusion-depletion code.

Table 1: Core design parameters of a supercritical CO_2 cooled fast reactor.

Power Output (MW)		Blanket Thickness (mm)	
Electric/Thermal	243.8/600	Axial/Radial	200 / 330.9
Cycle Efficiency (%)	40.6		
Coolant (Inlet/Outlet)		Subassembly Geometry (mm)	
Temperature (°C)	388/527	Pitch	182
Pressure (MPa)	12.8/12.5	Duct Thickness	3.5
Materials		Core Fuel Pin	
Coolant	CO_2	Number per Subassembly	391
Fuel	UO_2-PuO_2-NpO_2	Outer Diameter (mm)	6.5
Absorber (^{10}B = 90%)	B_4C	Cladding Thickness (mm)	0.35
Structural Material	316 SS	Spacing	Grid Spacer
		Pitch (mm)	8.45
Core Geometry (m)		Core Fuel Volume Ratio (%)	
Effective Core Height	1.200	Fuel	34.05
Equivalent Diameter	3.146	Structural Material	17.25
Pu Fissile Enrichment (%*)		Coolant	46.74
Inner Core/Outer Core	14.7 / 20.0	Gap	1.96

* Weight %

Neptunium-237 is added uniformly into the core fuel regions that transmute to ^{239}Pu in the core after two neutron capture reactions via ^{238}Pu, as given below.

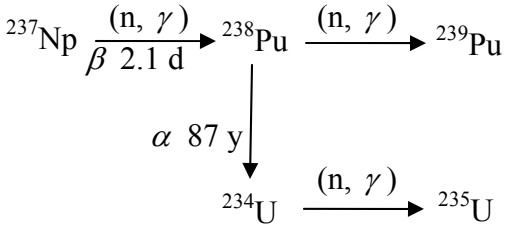

Therefore, ^{237}Np mainly functions as a neutron absorber in the early stage and a fissile material in the later stage. Figures 2 and 3 show that the core can be burned for 10 years without refueling and burnup reactivity loss, which is defined as k_{eff} difference from the beginning of cycle (BOC) to the end of cycle (EOC), is reduced to the rate of 0.02% $\Delta k/k$ per ten years by adding 6.5 weight percent content of ^{237}Np into the fuel as a burnable poison, while the maximum reactivity swing, which is defined as the difference between the maximum k_{eff} and the minimum k_{eff} over the cycle time, is 0.14% $\Delta k/k$. After ten-year burning, all core fuel and blanket fuel are discharged and fresh fuel is loaded. The maximum neutron flux level in the core is about five times lower than that of a usual sodium-cooled reactor, e.g., MONJU. Therefore, fast neutron fluence (≥0.1 MeV) does not become greater than its maximum permissible value for the core structural material of

MONJU, mainly because of its approximately five times lower power density. Such lower power density is required for maintaining sufficient heat transfer performance in the CO_2 cooled core and is the direct result of core height elongation from 0.93 m to 1.2 m, equivalent core diameter increase from 1.79 m to 3.15 m, and thermal power difference from 714 MW to 600 MW, compared with those of MONJU.

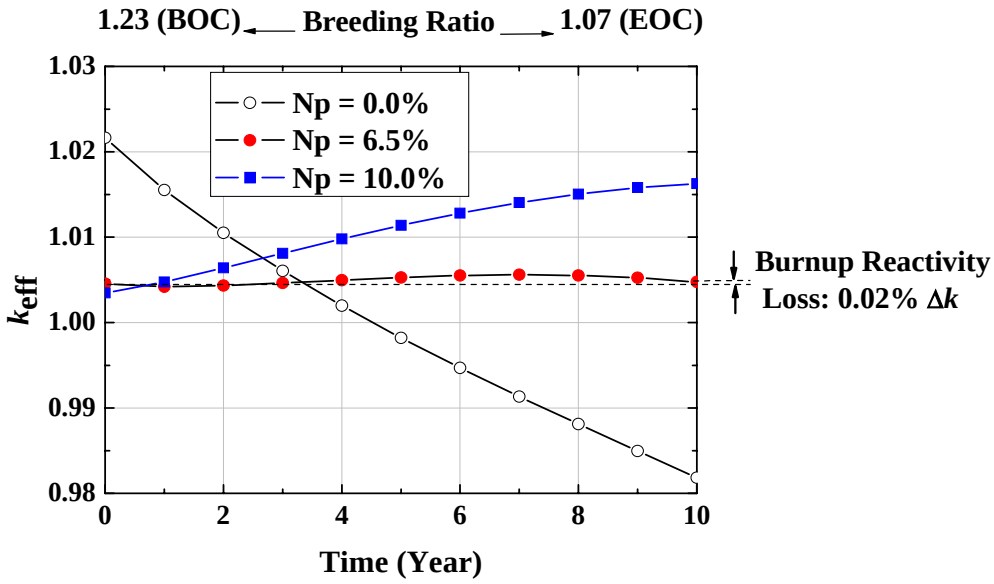

Figure 2: Burnup performance with ^{237}Np content

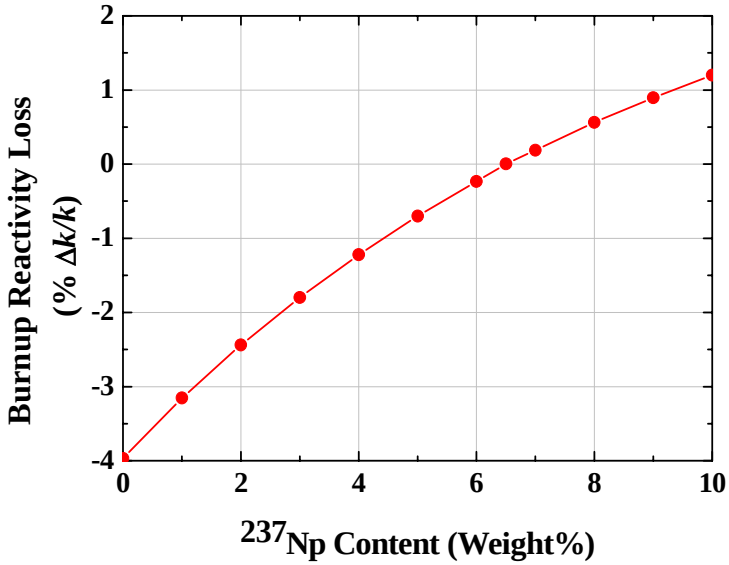

Figure 3: Dependence of ^{237}Np content on burnup reactivity loss

Reactivity worth requirements for both the primary and backup control rods are listed in Table 2. Seven primary control rods with a one-rod stuck condition offer a minimal shutdown margin of 3.7% $\Delta k/kk$', which is considered adequate, and the backup control

system provides a larger shutdown margin. Approximately zero burnup reactivity engenders great reduction in control rod worth requirements for primary rods. As a case in contrast, MONJU, with an electrical output of 280 MWe, has 13 primary rods and 6 backup rods. The number of control rods is reduced to half that of MONJU in all numbers. Rod withdrawal operations with burnup time to compensate the reactivity loss are almost unnecessary. Moreover, the excess reactivity is minimized so the core can be kept critical under consideration of the reactivity uncertainty. Primary rods are withdrawn from the core during the operation and reactivity insertion from rod withdrawal is very small.

Table 2: Control requirement and reactivity worth

Items	Primary Rods	Backup Rods
Number of Control Rods	7	3
Control Requirement (%$\Delta k/kk'$)		
Cold to Full Power Reactivity	0.6	0.6
Burnup Reactivity	0.3	-
Uncertainty	1.0	-
Allowance	0.3	-
Total	2.2	0.6
Reactivity Worth Available (%$\Delta k/kk'$)	5.9*	6.6
Shutdown Margin (%$\Delta k/kk'$)	3.7	6.0

* Worth of one-rod-stuck condition

The heavy metal inventory in the core at BOC and EOC is shown in Table 3. The total amount of ^{237}Np burned in the core is about 69 kg after ten years, which is equivalent to the quantity produced from about 14 LWRs of the same electrical output. Because ^{237}Np comprises about 40–60% of the total MAs discharged from PWRs and BWRs, it is a principal long-life radioactive wastes in MAs. Breeding ratios are about 1.23 at BOC and 1.07 at EOC. Void reactivity is about 0.72% $\Delta k/kk'$ at BOC and 0.38% $\Delta k/kk'$, which is calculated from the difference in effective multiplication factors when pressure is reduced from the rated value of 12.5 MPa to atmospheric pressure. The lower void reactivity at EOC relative to that at BOC is ascribed to the decrease of ^{237}Np in the core from BOC to EOC through its burning, as shown in Table 3. This void reactivity value is smaller by 25% than that of MONJU (2.5 \$=0.9% $\Delta k/kk'$) although ^{237}Np is added by content of 6.5 weight percent into the core fuel and the active core length (1.2 m) is longer by 0.27 m relative to that of MONJU (0.93 m). In sodium-cooled FRs, instantaneous reactivity insertion must be assumed in accident events because core voiding might occur instantaneously when gas enters or if the coolant boils. In contrast, core voiding occurs gradually at the speed of depressurization; the pressure half reduction time is about 10 min in the case of CO_2, as shown in Fig. 4, based on a simple model [12]. According to depressurization transient analysis instead of the simple model, the half reduction time is about 16 min. Therefore, the primary control rods have sufficient time to be inserted for compensation of the void reactivity, not only by the shutdown mechanism with scram time of about one minute, but also by the regular control rod drive mechanism.

The radial power distribution at the core midplane at BOC and EOC is shown in Fig. 4. The maximum power density in the inner core increases by about 10%. That in the outer core decreases by about 20% from BOC to EOC. The variation ranges from BOC to EOC are comparable in percentage with those of the usual sodium-cooled mix oxide core, in which ^{237}Np is not added. Fissile plutonium enrichment has been determined so that the maximum power density in the inner core matches that in the outer core because the plutonium enrichment is known empirically to maximize the average power density over a whole core in the case of a two-region core. The axial power distribution at the inner core fuel subassembly having maximum power density at BOC is shown in Fig. 5.

Table 3: Change of the heavy metal nuclide inventory

Nuclide	Inventory of Heavy Metal Nuclides (ton)		
	BOC	EOC	Inventory Change
^{235}U	0.147	0.099	-0.048
^{238}U	48.739	46.207	-2.532
Total U	**48.886**	**46.306**	**-2.580**
^{237}Np	1.828	1.141	-0.687
Total Np	**1.828**	**1.141**	**-0.687**
^{238}Pu	0.080	0.507	0.427
^{239}Pu	2.745	3.349	0.604
^{240}Pu	1.181	1.221	0.040
^{241}Pu	0.435	0.218	-0.217
^{242}Pu	0.222	0.214	-0.008
Total Pu	**4.663**	**5.509**	**0.846**
^{241}Am	0.061	0.153	0.092
^{242m}Am	0.000	0.006	0.006
^{243}Am	0.000	0.020	0.020
Total Am	**0.061**	**0.179**	**0.118**
^{242}Cm	0.000	0.003	0.003
^{244}Cm	0.000	0.004	0.004
Total Cm	**0.000**	**0.007**	**0.007**

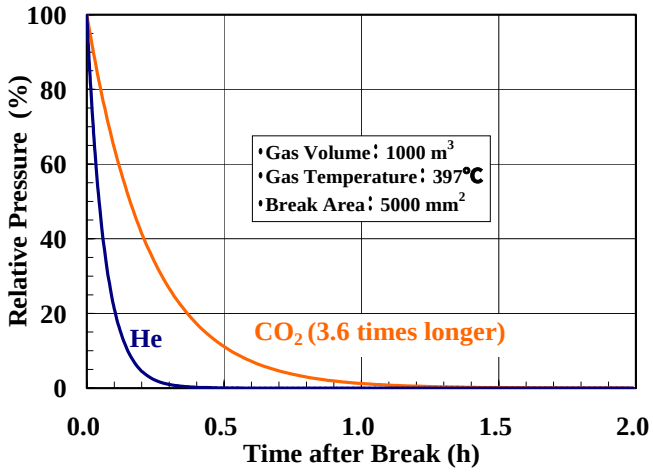

Figure 4: Pressure transient for a depressurization accident

According to the radial power distribution shown in Fig. 5, the core fuel subassemblies are grouped concentrically into seven annular coolant orificing zones, as shown in Fig. 7, the coolant flow rate is varied by orificing zones to make the average coolant temperature as high as possible after mixing at the core outlet. The flow rate is adjusted so that fuel cladding of the hottest pin at each orificing zone gives almost the same maximum permissible temperature of 700°C in this study. The coolant flow rate is given in Table 4.

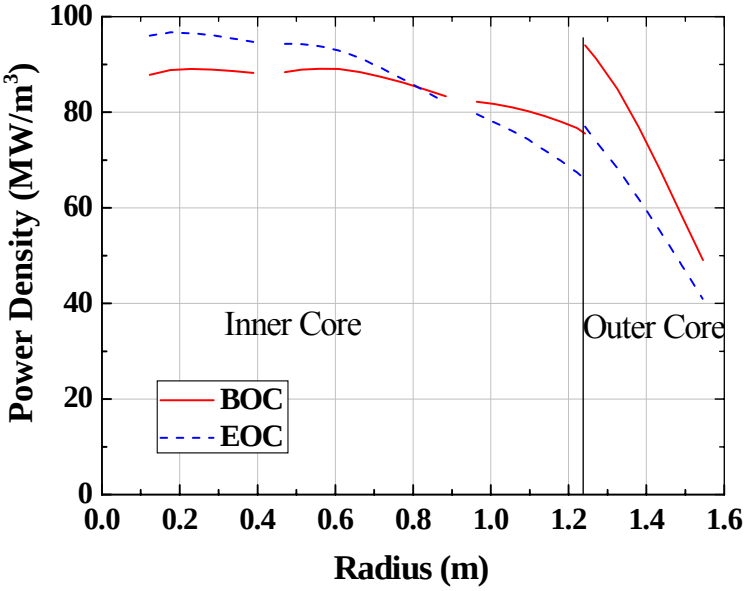

Figure 5: Radial power distribution at the midplane

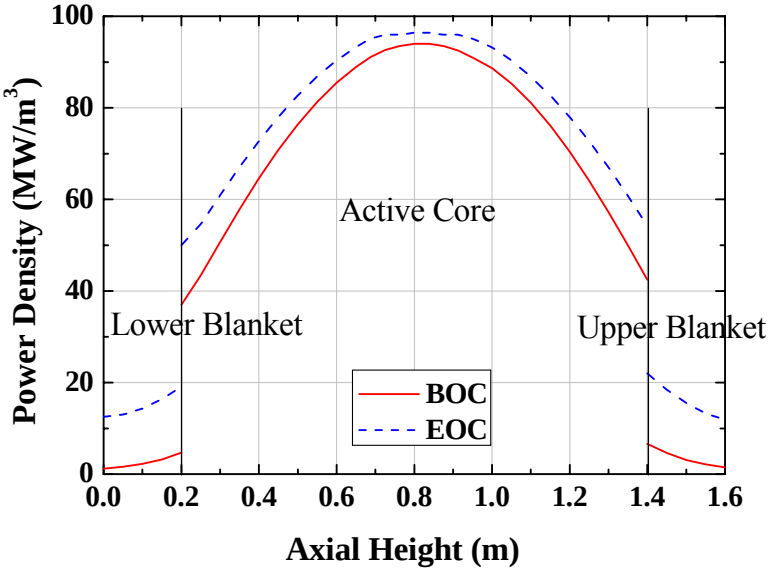

Figure 6: Axial power distribution in the core fuel assembly with maximum power density

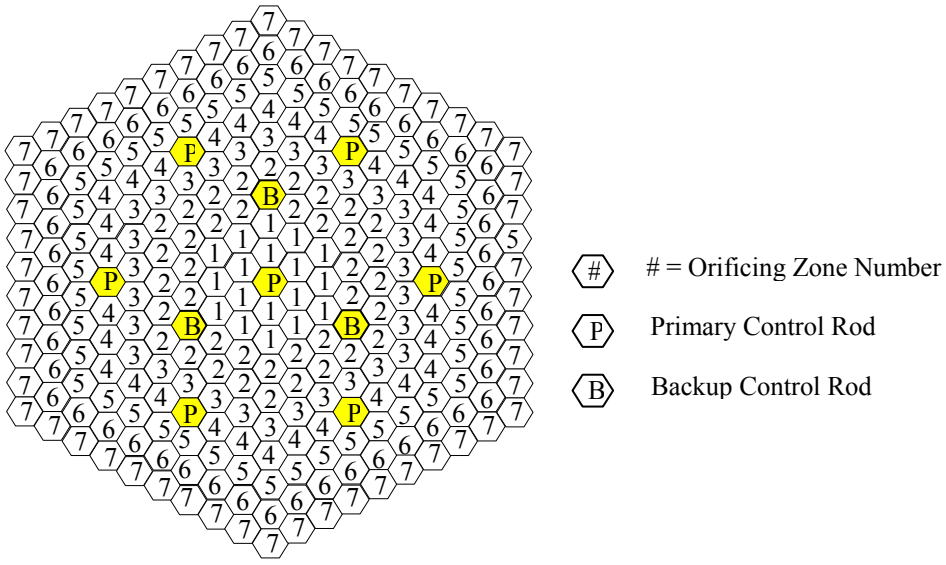

Figure 7: Coolant flow orificing zones in the core

Table 4: Coolant flow rate in orificing zones

Region Name	Orificing Zone Number	Total Number of Fuel Subassemblies	Coolant Flow Rate (kg/s Subassembly)
Inner Core	1	18	15.6
	2	39	15.2
	3	30	14.9
	4	30	12.8
	5	42	12.0
Outer Core	6	48	13.9
	7	54	10.7

Hot spot temperatures of fuel cladding are calculated, taking into account the uncertainties in evaluation by hot spot factors into nominal temperature obtained from subchannel analyses. The uncertainties are categorized as cumulative and statistical uncertainties. The total uncertainty F_c is written as

$$F_c = \prod_{i=1}^{m} F_c^i \,, \tag{1}$$

where F_c^i is the cumulative hot spot factor for hot spot effect i and m is the number of cumulative hot spot factors. The total statistical uncertainty F_s is given as

$$F_s = 1 + \left[\sum_{j=1}^{n} \left(F_s^j - 1 \right)^2 \right]^{1/2} , \tag{2}$$

where F_s^j is the statistical hot spot factor for a hot spot effect j, and n is the number of statistical hot factors. Using the above hot spot factors, the hot spot temperature of cladding is calculated as

$$T_l^{HS} = T_{in} + \sum_{k=1}^{l} \prod_{i=1}^{m} F_c^{i,k} \cdot \Delta T_k \left[\sum_{j=1}^{n} \left\{ \sum_{k=1}^{l} \left(F_s^{j,k} - 1 \right) \prod_{i=1}^{m} F_c^{i,k} \cdot \Delta T_k \right\}^2 \right]^{1/2}, \quad (3)$$

where T_l^{HS} is the hot spot temperature at l (= 1, …, 5) with 1 = coolant, 2 = fuel cladding outer surface, 3 = fuel cladding inner surface, 4 = fuel pellet outer surface, and 5 = fuel pellet center. ΔT_k is the nominal temperature rise across k (= 1, …, 5) with 1 = coolant, 2 = film between the coolant and fuel cladding outer surface, 3 = fuel cladding outer to inner surface, 4 = gap between fuel cladding inner surface to fuel pellet outer surface, and 5 = fuel pellet surface to center.

In the present study, the nominal temperatures were calculated using a subchannel analysis code DIANA [13]. The hotspot factors that are listed in Table 5 were applied to the nominal temperatures. The resulting hot spot temperature of cladding is below the maximum permissible temperature (700°C) of the core structural material developed for MONJU (SUS316FR).

Table 5: Hot spot factors

Items	Hot Spot Factor		
	Coolant	Film	Cladding
Direct			
Power Measurement	-	1.03	1.03
Power Distribution	1.08	1.08	1.08
Inlet Temperature	1.02	-	-
Subchannel Flow	1.02	-	-
Total	1.12	1.11	1.11
Statistical			
Flow Distribution	1.02	-	-
Coolant Property	1.02	1.30	1.03
Manufacturing	1.03	1.04	1.06
Pellet Eccentricity	-	1.16	1.20
Total	1.04	1.34	1.21

3. Conclusion

When ^{237}Np is added to the core of a supercritical CO_2 cooled fast reactor at content of 6.5%, ^{237}Np burns the equivalent quantity of fuel, with the same electrical output produced from about 14 LWRs. The burnup reactivity loss becomes essentially zero of the rate of 0.02% $\Delta k/k$ over ten years. The control rod number is reduced to half that of a usual sodium-cooled mixed fuel core with no added ^{237}Np. Void reactivity is smaller by about 25% than that of a usual core, even though ^{237}Np is added and the active core length is elongated to 1.2 m. The hot spot temperature of cladding is below its maximum permissible temperature of 700°C.

References

1. A. E. Walter and A. B. Reynolds, "Fast Breeder Reactors," *Pergamon Press*, pp. 705-706 (1981).
2. C. P. Gratton, "The Gas-Cooled Fast Reactor in 1981," *Nuclear Energy*, **20**, pp. 287-295 (1981).
3. Y. Kato, T. Nitawaki and Y. Yoshizawa, "A Carbon Dioxide Partial Condensation Direct Cycle for Advanced Gas cooled Fast and Thermal Reactors," *Proc. Int. Conf. on Back-End of the Fuel Cycle: From Research to Solutions (GLOBAL 2001),* Paris, France, September 9–13, 2001, Paper #028 (2001).
4. Y. Kato, T. Nitawaki and Y. Muto, "Medium Temperature Carbon Dioxide Gas Turbine Reactor," *Nucl. Eng. Design*, **230**, pp. 195-207 (2004).
5. V. Dostal, M. J. Driscol, P. Hejzlar, and N. E. Todreas, "A Supercritical CO_2 Gas Turbine Power Cycle for Next-Generation Nuclear Reactors," *Proc. 10th Intl. Conf. on Nuclear Engineering (ICONE-10)*," Virginia, USA, April 14–18, 2002, ICONE10-22192 (2002).
6. Y. Muto, T. Nitawaki and Y. Kato, "Comparative Design Study of Carbon Dioxide Gas Turbine and Helium Gas Turbine for HTGR Power Plant," *Proc. 2003 Intl. Congress on Advanced Nuclear Power Plants (ICAPP'03)*, Cordoba, Spain, May 4–7, 2003, Paper #3260.
7. Y. Muto and Y. Kato, "Turbomachinery Design of Supercritical CO_2 Gas Turbine Fast Reactor," *Proc. 2006 Intl. Congress on Advanced Nuclear Power Plants (ICAPP'06)*, Reno, Nevada, USA, June 4–8, Paper #6094, 2006.
8. M. Salvatores, A. Zaetta, C. Girad, M. Delpech, I. Slessarev, and J. Tommasi, "Nuclear Waste Transmutation," *Appl. Radiat. Isot*., **46**, pp. 681-687 (1995).
9. M. Yamaoka and T. Wakabayashi, "Study on Supper-long-life Cores Loaded with Minor Actinide Fuel," *Nucl. Eng. Design*, **154**, pp. 239-250 (1995).
10. M. Salvatores, "Nuclear Fuel Cycle Strategies Including Partitioning and Transmutation," *Nucl. Eng. Design*, **235**, pp. 805-816 (2005).
11. I. Y. Krivitski, M. F. Vorotyntsev, V. K. Pyshin, and L. V. Korobeinikova, "Neutronic and Safety Aspects of Inert Matrix Fuel Utilization in Fast Reactors for Plutonium and Minor Actinides Transmutation," *Progress Nucl. Energy*, **38**, pp. 391-394 (2001).
12. E. E. Lewis, "*Nuclear Power Reactor Safety*," John Wiley & Sons, pp. 398-402 (1977).
13. S. Hirao and N. Nakao, "Diana: a Fast and High Capacity Computer Code for Interchannel Coolant Mixing in Rod Arrays," *Nucl. Eng. Design*, **30**, pp. 214-222 (1974).